

When Pigs Fly: Contextual Reasoning in Synthetic and Natural Scenes

Philipp Bomatter^{1,*}, Mengmi Zhang^{2,3,*}, Dimitar Karev⁴, Spandan Madan^{3,5}, Claire Tseng⁴, and Gabriel Kreiman^{2,3}

*Equal contribution

Address correspondence to gabriel.kreiman@tch.harvard.edu

¹ETH Zürich

²Children’s Hospital, Harvard Medical School

³Center for Brains, Minds and Machines

⁴Harvard College, Harvard University

⁵School of Engineering and Applied Sciences, Harvard University

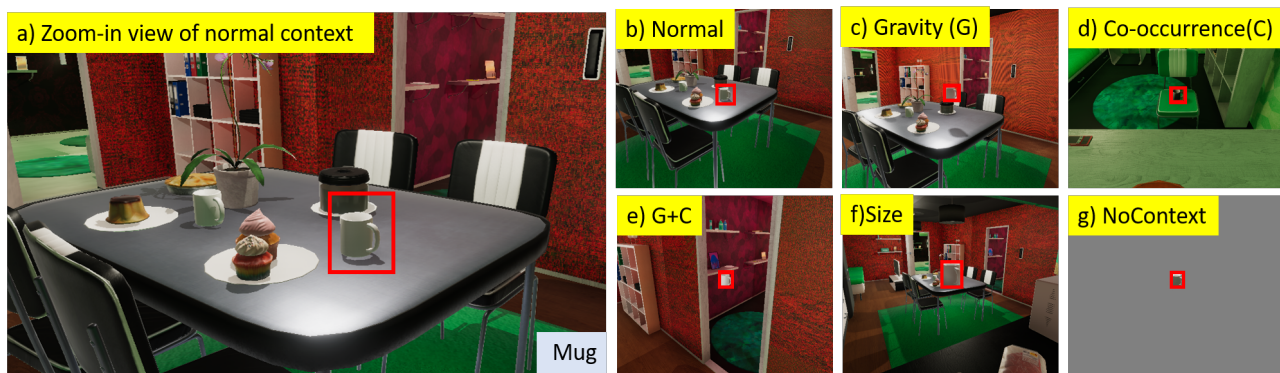


Figure 1: **Images under normal context and out-of-context conditions were generated in the VirtualHome environment [28] using the Unity 3D simulation engine [20].** One set of examples is shown. The same target object (a mug indicated by the red bounding box) is shown in different context conditions: normal context and out-of-context conditions including gravity (target object is floating in the air), object co-occurrence statistics, combination of both gravity and object co-occurrence statistics, enlarged object size, and no context with uniform grey pixels as background.

Abstract

Context is of fundamental importance to both human and machine vision—an object in the air is more likely to be an airplane, than a pig. The rich notion of context incorporates several aspects including physics rules, statistical co-occurrences, and relative object sizes, among others. While previous works have crowd-sourced out-of-context photographs from the web to study scene context, controlling the nature and extent of contextual violations has been an extremely daunting task. Here we introduce a diverse, synthetic Out-of-Context Dataset (OCD) with fine-grained control over scene context. By leveraging a 3D simulation engine, we systematically control the gravity, object co-occurrences and relative sizes across 36 object categories in a virtual household

environment. We then conduct a series of experiments to gain insights into the impact of contextual cues on both human and machine vision using OCD. First, we conduct psycho-physics experiments to establish a human benchmark for out-of-context recognition, and then compare it with state-of-the-art computer vision models to quantify the gap between the two. Finally, we propose a context-aware recognition transformer model, fusing object and contextual information via multi-head attention. Our model captures useful information for contextual reasoning, enabling human-level performance and significantly better robustness in out-of-context conditions compared to baseline models across OCD and other existing out-of-context natural image datasets. All source code and data are publicly available <https://github.com/kreimanlab/WhenPigsFlyContext>.

1. Introduction

A coffee mug is usually a small object (Fig.1a). It does not fly on its own (Fig.1c), and can often be found on a table (Fig.1a), and not on a chair (Fig.1d). Such contextual cues have a pronounced impact on the object recognition capabilities of both humans [41], and computer vision models [36, 8]. Neural networks learn co-occurrence statistics between an object’s appearance and its label, but also between the object’s context and its label [12, 32, 2]. Therefore, it is not surprising that recognition models fail to recognize objects in unfamiliar contexts [30].

Despite the fundamental role of context in visual recognition, it remains unclear *what* and *how* contextual cues should be integrated with object information. Large-scale, internet-scraped datasets like ImageNet [10] are highly uncontrolled, which makes it hard to quantify how context affects recognition. To address this challenge, here we present a methodology to systematically study the effects of an object’s context on recognition by leveraging a Unity-based 3D simulation engine for image generation [20], and manipulating 3D objects in a virtual home environment [28]. The ability to rigorously control every aspect of the scene enables us to systematically violate contextual rules and assess their impact on recognition.

We focus on three fundamental aspects of context: (1) *gravity* - objects without physical support, (2) *object co-occurrences*, and (3) *relative size* - changes to the size of target objects relative to the background. In contrast to existing out-of-context real-world photographs, our approach provides fine-grained control to alter one aspect of context at a time, and the flexibility to modify various aspects of context including 3D geometric transformations, locations, viewpoints, and materials. We use these generated images to gain insights into how contextual cues impact object recognition in humans and state-of-the-art computer vision models.

Our contributions in this paper are three-fold. Firstly, we introduce a challenging new dataset for in- and out-of-context object recognition that allows fine-grained control over context violations including gravity, object co-occurrences and relative object sizes (*out-of-context dataset*, OCD). Secondly, we conduct psycho-physics experiments to establish a human benchmark for out-of-context recognition and compare it with state-of-the-art computer vision models, thus quantifying the gap between human and computer vision. Finally, we propose a new context-aware architecture for object recognition which can incorporate object and contextual information to reason in context and also generalize well to out-of-context images. Our Context-aware Recognition Transformer Network (*CRTNet*) uses two separate streams to process the object and its context independently before integrating them via multi-head attention in transformer

decoders. The model then makes a classification decision by weighting these two streams based on a predicted confidence score. Across multiple datasets, we demonstrate that the CRTNet model surpasses other state-of-the-art computational models and classifies objects more robustly despite large contextual variations, much like humans do.

2. Related Works

Out-of-context object recognition: Context is of incredible importance to machine vision models for object recognition [26, 23]. Deep networks trained on natural image datasets like *e.g.* ImageNet [21] rely implicitly but strongly on context [15, 4, 31]. Indeed, these algorithms often fail when objects are placed in an incongruent context. Most work in the literature have represented context as a monolithic property in the form of the target object’s background. This includes testing the generalization to new backgrounds [2], incongruent backgrounds [41], exploring impact of foreground-background relationships on data augmentation [14], and replacing image sub-regions by another sub-image *i.e.* object transplanting [30]. To the best of our knowledge, there is no existing work exploring aspects of object context (*e.g.* gravity) in a quantitatively controlled, systematic manner as done in this paper.

3D simulation engines and computer vision: Recent works have demonstrated the success of using 3D virtual environments for tasks such as object recognition with simple and uniform backgrounds [3], routine program synthesis [28], 3D animal pose estimation [25], and for studying the generalization capabilities of CNNs [24, 17]. However, to the best of our knowledge, none of these studies have tackled the challenging problem of contextual modulation. Compared with other works on contextual effects on a set of limited number of natural images [27, 30], 3D simulation engines allow us to easily synthesize as many pictures as possible and violate contextual rules, which is impractical to achieve with real-world photographs. Moreover, these simulation engines also enable us to control contextual parameters precisely such that we can vary one at a time in a systematic and quantifiable manner.

Models for context-aware object recognition: To tackle the problem of context-aware object recognition, researchers have proposed classical approaches, *e.g.* Conditional Random Field (CRF) [16, 40, 22, 7], and graph-based methods [34, 39, 35, 8]. Recent works have extended this line of work to deep graph neural networks [18, 9, 11, 1]. Breaking away from these previous works where graph optimization is performed globally for contextual reasoning in object recognition, our model has a two-stream architecture which separately processes visual information on both target objects and context, and then integrates them with multi-head attention in stacks of transformer decoding layers. Contrasting other vision

transformer models in object recognition [13] and detection [6], CRTNet performs in-context recognition tasks given the target object location.

3. Context-aware Recognition Transformer

3.1. Overview

We propose the Context-aware Recognition Transformer Network (CRTNet, Figure 2) and introduce three novel designs in CRTNet: First, CRTNet involves transformer decoder modules for integrating object and contextual information to reason about context via stacks of multi-headed encoder-decoder attention. Second, we introduce a confidence-weighting mechanism that improves the model’s robustness and gives it the flexibility to select what information to rely on for recognition. Third, we curated the training methodology with gradient detachment to prioritize important model components and ensure efficient training of the entire architecture.

CRTNet is presented with an image with multiple objects and a bounding box to indicate the target object location. Inspired by the eccentricity dependence of human vision, CRTNet has one stream that processes only the target object (I_t , 224×224), and a second stream devoted to the periphery (I_c , 224×224). I_t is obtained by cropping the input image to the bounding box whereas I_c covers the entire contextual area of the image. I_c and I_t are then resized to the same dimensions. Thus, the target object’s resolution is higher in I_t . The two streams are encoded through two separate 2D-CNNs. After the encoding stage, CRTNet tokenizes the feature maps of I_t and I_c , integrates object and context information via hierarchical reasoning through a stack of transformer decoder layers, and predicts class label probabilities $y_{t,c}$ within C classes.

A model that always relies on context can make mistakes under unusual context. To increase robustness, CRTNet makes a second prediction y_t , based on target object information alone, estimates the confidence p of this prediction, and computes a confidence-weighted average of y_t and $y_{t,c}$ to get the final prediction y_p . If the model makes a confident prediction with the object only, it overrules the context reasoning stage.

3.2. Convolutional Feature Extraction

CRTNet takes I_c and I_t as inputs and uses two 2D-CNNs, $E_c(\cdot)$ and $E_t(\cdot)$, to extract context and target feature maps a_c and a_t , respectively, where $E_c(\cdot)$ and $E_t(\cdot)$ are parameterized by θ_{E_c} and θ_{E_t} . Concretely, we use the DenseNet architecture [19] with weights pre-trained on ImageNet [10] and fine-tune it. Assuming that different features in I_c and I_t are useful for recognition, we do not enforce sharing between the parameters θ_{E_c} and θ_{E_t} . We demonstrate the advantage of non-shared parameters in

the ablation study (Sec. 5.5). To allow CRTNet to focus on specific parts of the image and select features at those locations, we preserve the spatial organization of features and define a_c and a_t as the output feature maps from the last convolution layer of DenseNet. Both a_c and a_t are of size $D \times W \times H = 1,664 \times 7 \times 7$, where D , W and H denote the number of channels, width and height of the feature maps respectively.

3.3. Tokenization and Positional Encoding

We tokenize the context feature map a_c by splitting it into patches based on locations, following [13]. Each context token corresponds to a feature vector \mathbf{a}_c^i of dimension D at location i where $i \in \{1, \dots, L = H \times W\}$. To compute target token T_t , CRTNet aggregates the target feature map a_t via average pooling:

$$T_t = \frac{1}{L} \sum_{i=1, \dots, L} \mathbf{a}_t^i \quad (1)$$

To encode the spatial relations between the target token and the context tokens, as well as between different context tokens, we learn a positional embedding of size D for each location i and add it to the corresponding context token \mathbf{a}_c^i . For the target token T_t , we use the positional embedding corresponding to the location, within which the bounding box midpoint is contained. The positionally-encoded context and target tokens are denoted by z_c and z_t respectively.

3.4. Transformer Decoder

We follow the original transformer decoder [38], taking z_c to compute keys and values, and z_t to generate the queries in the transformer encoder-decoder multi-head attention layer. Since we only have a single target token, we omit the self-attention layer. In the experiments, we also tested CRTNet with self-attention enabled and we did not observe performance improvements. Our decoder layer consists of alternating layers of encoder-decoder attention (EDA) and multi-layer perceptron (MLP) blocks. Layernorm (LN) is applied after each residual connection. Dropout (DROP) is applied within each residual connection and MLP block. The MLP contains two layers with a ReLU non-linearity and DROP.

$$z_{t,c} = \text{LN}(\text{DROP}(\text{EDA}(z_t, z_c)) + z_t) \quad (2)$$

$$z'_{t,c} = \text{LN}(\text{DROP}(\text{MLP}(z_{t,c})) + z_{t,c}) \quad (3)$$

Our transformer decoder has a stack of $X = 6$ layers, indexed by x . We repeat the operations in Eqs 2 and 3 for each transformer decoder layer by recursively assigning $z'_{t,c}$ back to z_t as input to the next transformer decoding layer. Each EDA layer integrates useful information between the context and the target object with 8-headed selective attention. Based on accumulated information from all the

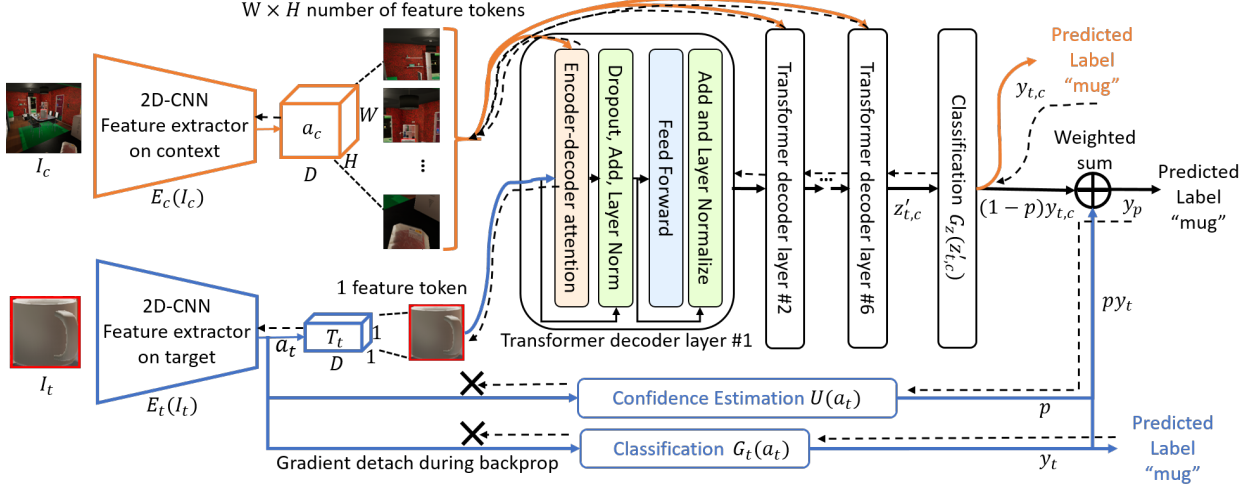


Figure 2: **Architecture overview of the Context-aware Recognition Transformer Network (CRTNet).** The diagram depicts the modular steps carried out by CRTNet in the context-aware object recognition task. CRTNet consists of 3 main modules: feature extraction, integration of context and target information, and confidence-modulated classification. CRTNet takes the cropped target object I_t and the entire context image I_c as inputs and extracts their respective features. These feature maps are then tokenized and the information of the two streams is integrated over multiple transformer decoding layers. CRTNet also estimates a confidence score of recognizing the target object based on object features alone, which is used to modulate the contributions of y_t and $y_{t,c}$ to the final prediction y_p . The dashed lines in backward direction denote gradient flows during backpropagation. The two black crosses denote where the gradient updates stop. See Sec. 3 for details.

previous $x - 1$ layers, each EDA layer enables CRTNet to progressively reason about context by updating the attention maps on z_c over all L locations and X layers. We provide visualization examples of attention maps along the hierarchy of the transformer decoder in Supp. Fig S1.

3.5. Confidence-modulated Recognition

The context classifier $G_z(\cdot)$ with parameters θ_{G_z} consists of a fully-connected layer and a *softmax* layer. It takes the feature embedding $z'_{t,c}$ from the last transformer decoder layer and outputs the predicted class distribution vector: $y_{t,c} = G_z(z'_{t,c})$. Similarly, the target classifier $G_t(\cdot)$, takes the feature maps a_t as input and outputs the predicted class distribution vector: $y_t = G_t(a_t)$.

Since neural networks are often fooled by incongruent context [41], we propose a confidence-modulated recognition mechanism balancing the predictions from $G_t(\cdot)$ and $G_z(\cdot)$. The confidence estimator $U(\cdot)$ with parameters θ_U takes the target feature map a_t as input and outputs a value p indicating how confident CRTNet is about the prediction y_t . $U(\cdot)$ is a feed-forward multi-layer perceptron network with a sigmoid function to normalize the confidence score to $[0, 1]$.

$$p = \frac{1}{1 + e^{-U(a_t)}} \quad (4)$$

We then use p to compute a confidence-weighted average of $y_{t,c}$ and y_t for the final predicted class distribution y_p : $y_p = py_t + (1 - p)y_{t,c}$. The higher the confidence p , the

more CRTNet relies on the target object itself rather than the integrated contextual information for classification. We demonstrate the advantage of using y_p rather than $y_{t,c}$ or y_t as a final prediction in the ablation study (Sec. 5.5).

3.6. Training

CRTNet is trained end-to-end with three cross-entropy losses introduced below: (i) to train the confidence estimator $U(\cdot)$, we use a cross-entropy loss with respect to the confidence-weighted prediction y_p . Intuitively, this allows $U(\cdot)$ to learn to increase the confidence value p for samples where the prediction y_t , based on target object information alone, tends to be correct. (ii) To train $G_t(\cdot)$, we use a cross-entropy loss with respect to y_t . (iii) For the rest of components in CRTNet including the transformer decoder and classifier $G_z(\cdot)$, we use a cross-entropy loss with respect to $y_{t,c}$. Instead of training everything based on y_p , the three cross-entropy losses altogether maintain strong learning signals for all parts in the architecture irrespective of the confidence value p .

To facilitate learning for specific components in CRTNet, we also introduced gradient detachments during backpropagations (Fig. 2). Gradients flowing through both $U(\cdot)$ and $G_t(\cdot)$ are detached from $E_t(\cdot)$ to prevent them from driving the target encoder to learn more discriminative features, which could impact the efficacy of the transformer modules and $G_z(\cdot)$. We demonstrate the benefit of these design decisions in ablation studies (Sec. 5.5).

4. Experimental Details

4.1. Baselines

We compared CRTNet against several baselines:

CATNet [41] is a context-aware two-stream object recognition model. It processes the visual features of cropped target object and context in parallel, dynamically incorporates object and contextual information by constantly updating its attention over image locations, and sequentially reasons about the class label for the target object via a recurrent neural network.

Faster R-CNN [29] is an object detection algorithm. We adapted it to the context-aware object recognition task by replacing the region proposal network with the ground truth bounding box indicating the location of the target object.

DenseNet [19] is a 2D-CNN with dense connections that takes the cropped target object patch I_t as input.

4.2. Datasets

4.2.1 In- and Out-of-context Dataset (OCD)

Our out-of-context dataset (OCD) contains 36 object classes, with 15,773 testing images in 6 contextual conditions. We leveraged the VirtualHome environment [28] developed in the Unity simulation engine to synthesize these images in indoor home environments within 7 apartments and 5 rooms per apartment. These rooms include furnished bedrooms, kitchens, study rooms, living rooms and bathrooms [28] (see Fig. 1 for examples). We extended VirtualHome with additional functionalities to manipulate object properties, such as materials and scales, and to place objects in out-of-context locations. The target object is always centered in the camera view. Collision checking and camera ray casting are enabled to prevent object collisions and occlusions.

To our best knowledge, our OCD is the first large dataset tackling the problem of contextual modulation in object recognition. Different from large-scale image classification datasets, such as ImageNet [10] where one single large object is typically centered on an image, our OCD involves highly complex and rich scenes with multiple objects in an image. Our OCD enables us to study context-aware recognition on both humans and models in a systematic and quantifiable manner. The far-from-perfect results (Sec. 5) demonstrate that our challenging OCD provides great venues to improve our current recognition models.

Normal Context and No Context: There are 2,309 images for normal context (Fig. 1b), and 2,309 images for no-context condition (Fig. 1g). For the normal context condition, each target object is placed in its “typical” location, defined by the default settings of VirtualHome. Then we generate a corresponding no context image for every normal context image by replacing all the pixels

surrounding the target object with either uniform grey pixels or salt and pepper noise.

Gravity: We generated 2,934 images where we move the target object along the vertical direction such that it is no longer supported (Fig. 1c). To avoid cases where objects are lifted so high that their surroundings change completely, we set the lifting offset to 0.25 meters.

Object Co-occurrences: To examine the importance of the statistics of object co-occurrences, four human subjects were asked to indicate the most likely room and location for the target objects. We use the output of these responses to generate 1,453 images where we place the target objects on surfaces with lower co-occurrence probability, e.g. a microwave in the bathroom and Fig. 1d.

Object Co-occurrences + Gravity: We generated 910 images where the objects are both lifted and placed in unlikely locations. We chose walls, windows, and doorways of rooms where the target object is typically absent (Fig. 1e). We place target objects at half of the apartment’s height.

Size: We created 5,858 images where we change the target object size to 2, 3, or 4 times its original size while keeping the remaining objects in the scene intact (Fig. 1f).

4.2.2 Real-world Out-of-context Datasets

The Cut-and-paste Dataset [41] contains 2,259 out-of-context images spanning 55 object classes. These images are grouped into 16 conditions obtained through the combinations of 4 object sizes and 4 context conditions (normal, minimal, congruent, and incongruent) (Fig. 3b).

The UnRel [27] **Dataset** contains more than 1,000 images with unusual relations among objects spanning 100 object classes. The dataset was collected from the web based on triplet queries, such as “dog rides bike” (Fig. 3c).

4.3. Performance Evaluation

Evaluation of Computational Models: We trained the models on natural images from COCO-Stuff [5] using the annotations for object classes overlapping with those in the respective test set (16 overlapping classes between VirtualHome and COCO-Stuff, 55 overlapping classes between Cut-and-paste and COCO-Stuff and 33 overlapping classes between UnRel and COCO-Stuff). These models were then tested on all six VirtualHome conditions, the Cut-and-paste Dataset, UnRel, and on a COCO-Stuff test split.

Behavioral Experiments: As a benchmark, we evaluated human recognition in the 6 contextual conditions described above (Sec. 4.2.1, Fig. 1), as schematically illustrated in Fig. 3d, on Amazon Mechanical Turk (MTurk) [37]. We recruited 400 subjects per experiment, yielding $\approx 67,000$ trials. To avoid biases and potential memory

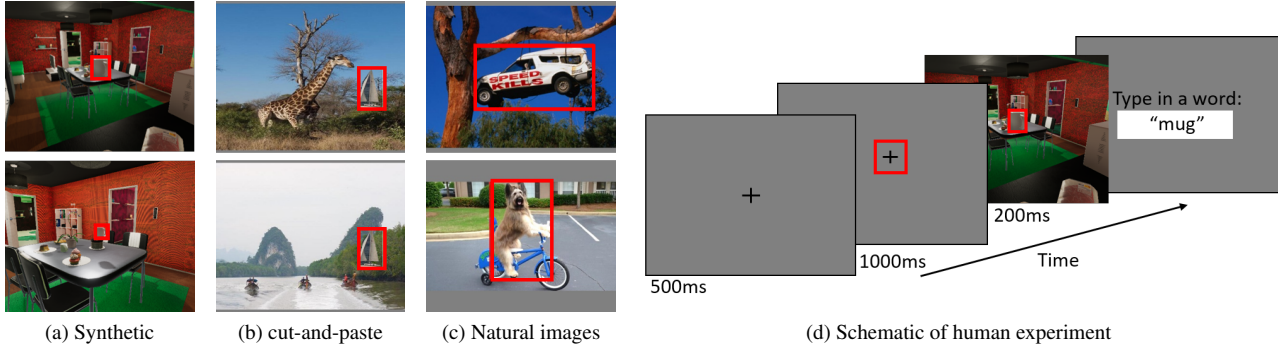


Figure 3: **Three out-of-context datasets and human benchmark experiment.** (a-c) Two example images from each out-of-context dataset. The red box shows the target location. In (a), two contextual modifications (gravity and size) are shown and the target object is always in the center. (b) Cut-and-paste dataset created from [41]. The same target object is cut and pasted in either incongruent or congruent conditions. The target object location is always the same across both conditions. (c). UnRel dataset [27]. There are no controlled conditions for comparison as (a) and (b). See Sec. 4 for further details. (d) Subjects were presented with a fixation cross (500 ms), followed by a bounding box indicating the target object location (1000 ms). The image was shown for 200 ms. After image offset, subjects typed one word to identify the target object. The correct answer (here, “mug”) is not shown in the actual experiment).

effects, we took several precautions: (a) Only one target object from each class was selected; (b) Each subject saw each room only once; (c) The trial order was randomized.

Computer vision and most psychophysics experiments enforce N-way categorization (e.g., [33]). Here we used a more unbiased probing mechanism whereby subjects could use any word to describe the target object. We independently collected ground truth answers for each object in a *separate* MTurk experiment with infinite viewing time and normal context conditions. These Mturk subjects did *not* participate in the main experiments. Answers in the main experiments were correct if they matched any of the ground truth responses [41]. Although computational models are evaluated using N-way categorization, we find it instructive to report model results alongside human behavior for comparison purposes. We also show human-model correlations to describe their relative trends across all conditions.

5. Results

5.1. Recognition in our OCD dataset

Figure 4 (left) reports recognition accuracy for humans over the 6 context conditions (Sec. 4.2.1, Fig. 1) and 2 target object sizes (total of 12 conditions). Comparing the no-context condition (white) versus normal context (black), it is evident that contextual cues lead to improvement in recognition, especially for smaller objects, consistent with previous work [41].

Gravity violations led to a reduction in accuracy. For small object, the gravity condition was even slightly worse than the no context condition; the unusual context can be

misleading for humans. The effects were similar for the changes in object co-occurrences and relative object size. Objects were enlarged by a factor of 2, 3, or 4 in the relative size condition. Since the target object gets larger, and because of the improvement in recognition with object size, we would expect a higher accuracy in the size condition compared to normal context. However, increasing the size of the target object while keeping all other objects intact, violates the basic statistics of expected relative sizes (e.g., we expect a chair to be larger than an apple). Thus, the drop in performance in the size condition is particularly remarkable and shows that violation of contextual cues can even override basic object recognition cues.

Combining changes in gravity and in the statistics of object co-occurrences led to a pronounced drop in accuracy. Especially for the small target objects, violation of gravity and statistical co-occurrences led to performance well below that in the no context condition.

These results show that context can play a facilitatory role (compare normal versus no context), but context can also impair performance (compare gravity+co-occurrence versus no context). In other words, unorthodox contextual information hurts recognition.

Figure 4 (right) reports accuracy for CRTNet. Adding normal contextual information led to an improvement of 4% (normal context vs no context) in performance for both small and large target objects. However, in contrast with humans (20% improvement in small objects versus 10% improvement in large objects), we did not observe the difference between the effect of contextual modulation for small versus large target objects for CRTNet. Remarkably, the CRTNet model qualitatively captured the effects of

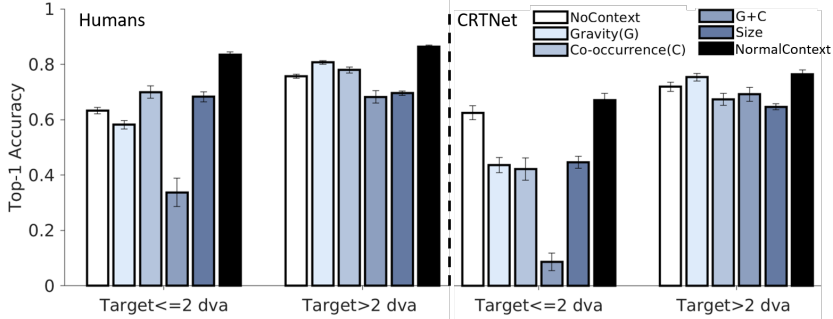


Figure 4: **Our CRTNet model exhibits human-like recognition patterns across contextual variations in our OCD dataset.** Different colors denote contextual conditions (Sec. 4.2.1, Fig. 1). We divided the trials into two groups based on target object sizes in degrees of visual angle (dva). Error bars denote standard error of the mean (SEM).

contextual violations. Overall, the performance of the model was below humans, particularly for small objects. However, the basic trends associated with the role of contextual information in humans can also be appreciated in the CRTNet results. Gravity, object co-occurrences, and relative object size changes led to a decrease in performance. As in the behavioral measurements, these effects were more pronounced for the small objects. For CRTNet, all conditions led to worse performance than the no context condition for small objects.

5.2. Recognition in Cut-and-paste

Synthetic images offer the possibility to systematically control every aspect of the scene, but these images still do not follow all the statistics of the natural world. Therefore, we evaluated whether CRTNet can generalize to naturalistic settings on the Cut-and-paste dataset [41]. For comparison, we reproduced the human psychophysics results in Table 2. The CRTNet model yielded results that were consistent, and in many conditions better than, human performance. As observed in the human data, performance increases with object size. In addition, the effect of context was more pronounced for smaller objects (compare normal context (NC) versus minimal context (MC) conditions).

Consistent with previous work [41], compared to the minimal context condition, congruent contextual information (CG) typically enhanced recognition whereas incongruent context (IC) impaired performance. Although the congruent context typically shares similar correlations between objects and scene properties, pasting the object in a congruent context led to weaker enhancement than the normal context. This lower contextual facilitation may be due to erroneous relative sizes between objects, unnatural boundaries created by pasting, or contextual cues specific to each image. CRTNet was relatively oblivious to these effects and performance in the congruent condition was closer to that in the normal context condition.

OCD	Overall
CRTNet (ours)	0.89
Baselines	
CATNet [41]	0.36
Faster R-CNN [29]	0.73
DenseNet [19]	0.66
Ablations	
Ablated-SharedEncoder	0.84
Ablated-TargetOnly	0.89
Ablated-Unweighted	0.83
Ablated-NoDetachment	0.88

Table 1: **Linear correlations between human and model performance over 12 contextual conditions.** Best is in bold.

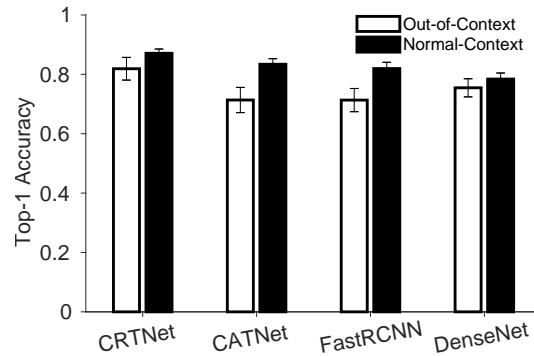


Figure 5: **Our CRTNet surpasses all baselines in both normal (COCO-Stuff [5]) and out-of-context (UnRel [27]) conditions.**

In stark contrast, the incongruent context consistently degraded recognition performance below the minimal context condition. While we observe similar trends for human and CRTNet, the absolute recognition accuracy of CRTNet was higher than human performance by $> 10\%$ across many of the context conditions.

5.3. Recognition in Natural Images

The Cut-and-paste dataset introduces artifacts (such as unnatural boundaries and erroneous relative sizes) due to the cut-and-paste process. Therefore, we next evaluated CRTNet on the UnRel dataset [27]. We use the performance on the COCO-Stuff [5] test split as reference for normal context in natural images. CRTNet showed a slightly lower recognition accuracy in the out-of-context setting (Fig. 5).

5.4. Comparison with baseline models

Performance Evaluation: Although Faster R-CNN and CATNet leverage global context information, CRTNet outperformed both models, especially on small objects (OCD: Table 1 and Supp. Fig. S7-S8; Cut-and-Paste: Table 2; UnRel: Fig. 5). CRTNet led CATNet by 7% and

	Size [0.5, 1] dva				Size [1.75, 2.25] dva				Size [3.5, 4.5] dva				Size [7, 9] dva			
	NC	CG	IG	MC	NC	CG	IG	MC	NC	CG	IG	MC	NC	CG	IG	MC
Humans [41]	56.0 (2.8)	18.8 (2.3)	5.9 (1.3)	10.1 (1.7)	66.8 (2.7)	48.6 (2.8)	22.3 (2.4)	38.9 (2.8)	78.9 (2.4)	66.0 (2.7)	38.8 (2.6)	62.0 (2.8)	88.7 (1.7)	70.7 (2.6)	59.0 (2.8)	77.4 (2.3)
CRTNet (ours)	50.2 (2.8)	43.9 (2.8)	10.6 (1.7)	17.4 (2.1)	78.4 (3.0)	81.4 (2.8)	41.2 (3.5)	56.7 (3.6)	91.5 (1.1)	87.3 (1.3)	51.1 (1.9)	76.6 (1.6)	92.9 (0.9)	87.7 (1.2)	66.4 (1.7)	83.0 (1.4)
CATNet [41]	37.5 (4.0)	29.2 (2.4)	3.6 (1.0)	6.1 (2.0)	53.0 (4.1)	46.5 (2.5)	10.9 (1.6)	22.1 (3.6)	72.8 (3.6)	71.2 (2.4)	24.5 (2.2)	38.9 (3.9)	81.8 (3.0)	78.9 (2.1)	47.6 (2.6)	74.8 (3.5)
Faster R-CNN [29]	24.9 (2.4)	10.9 (1.7)	5.9 (1.3)	7.2 (1.4)	44.3 (3.6)	27.3 (3.2)	20.1 (2.9)	16.5 (2.7)	65.1 (1.8)	53.2 (1.9)	39.0 (1.9)	42.9 (1.9)	71.5 (1.6)	64.3 (1.7)	55.0 (1.8)	64.6 (1.7)
DenseNet [19]	13.1 (1.9)	10.0 (1.7)	11.2 (1.8)	12.5 (1.8)	45.4 (3.6)	42.3 (3.5)	39.7 (3.5)	46.4 (3.6)	67.1 (1.8)	62.3 (1.9)	55.4 (1.9)	67.1 (1.8)	74.9 (1.6)	67.2 (1.7)	63.5 (1.7)	74.9 (1.6)

Table 2: **Recognition accuracy of humans, our model (CRTNet), and baselines on the Cut-and-paste Dataset [41].** There are 4 conditions for each size: normal context (NC), congruent context (GC), incongruent context (IC) and minimal context (MC) (Sec. 4.2.2). Bold highlights the best performance. Numbers in brackets denote standard error of the mean.

Faster R-CNN by 20% for normal context and [0.5,1] dva size in the Cut-and-paste dataset (Table 2; similar results for other experiments in Supp. Fig. S7-S8). CRTNet is also more similar to human performance by a large margin in OCD and the Cut-and-Paste datasets (Table 1 and 2).

Architectural Differences: While all baseline models can rely on an intrinsic notion of spatial relations, CRTNet learns about spatial relations between target and context tokens through a positional embedding. A visualization of the learned positional embeddings (Supp. Fig. S1) shows that CRTNet learns image topology by encoding distance within the image in the similarity of position embeddings.

In CATNet, the attention map iteratively modulates the extracted feature maps from the context image at each time step in a recurrent neural network, whereas CRTNet uses a stack of feedforward transformer decoding layers with multi-headed encoder-decoder attention. These decoding layers hierarchically integrate information via attention maps, modulating the target token features with context information. Transformer architectures also tend to perform better than recurrent neural networks in NLP [38] and computer vision tasks [13, 6].

DenseNet takes cropped targets as input with few surrounding pixels of context and outputs predicted labels. Its performance dramatically decreases for smaller objects, resulting in lower correlation with humans. For example, in the Cut-and-paste dataset, CRTNet outperforms DenseNet by 30% for normal context and small objects (Table 2) and in OCD, DenseNet shows a correlation of 0.66 with human performance (vs. 0.89 for CRTNet, Table 1).

5.5. Ablation Reveals Critical Model Components

We assessed the importance of design choices by training and testing ablated versions of CRTNet on OCD dataset.

Shared Encoder: In our CRTNet model, we trained two separate encoders, $E_t(\cdot)$ and $E_c(\cdot)$, to extract features from target objects and the context respectively. Here, we enforced weight-sharing between these two encoders (Ablated-SharedEncoder) to assess whether the features

relevant for target object recognition are different from those used in contextual reasoning. The ablation results (Table 1, Supp. Fig. S3) show that CRTNet with a shared encoder achieved a lower recognition accuracy and lower correlation with the psychophysics results.

Recognition Based on Target or Context Alone: During testing, we use the confidence-weighted prediction y_p as the final prediction. Here, we considered two extreme cases: CRTNet relying only on the target object itself (y_t , Ablated-TargetOnly) and CRTNet relying only on contextual reasoning ($y_{t,c}$, Ablated-Unweighted). The original model outperforms either of these ablated scenarios (Table 1 and Supp. Figs S4 and S5). This suggests that a confidence-modulated classification mechanism is essential for recognition models to be adaptive and robust given contextual variations.

Joint Training of the Target Encoder: In Sec. 3.6, we make the training of the target encoder $E_t(\cdot)$ independent of $G_t(\cdot)$ such that it can not force the target encoder to learn more discriminative features. In this ablated model, we remove this detaching constraint and train the target encoder $E_t(\cdot)$ jointly (Ablated-NoDetachment, Table 1 and Supp. Fig. S6). The results are inferior to the ones of our original CRTNet, implying that detaching of the target encoder is helpful for recognition.

6. Discussion

We quantitatively studied the role of context in visual recognition in humans and computational models. We introduce a dataset (OCD) consisting of 15,773 images to systematically study out-of-context objects in simulated indoor home environments. We investigated the role of gravity, object co-occurrences, and relative object sizes in object recognition. As an essential benchmark, we tested both humans and models on this dataset. Since these synthetic images can still be easily distinguished from real photos, the domain gap might influence the recognition performance. To further test the generalization of humans

and models, we consider out-of-context variations in two datasets consisting of real photographs. We show consistent results over all three datasets that contextual cues can enhance visual recognition, but the “wrong” context can also impair visual recognition, both for humans and models.

We proposed a context-aware recognition transformer model that integrates contextual and object cues via multi-head transformer decoding layers. To increase robustness in visual recognition, we introduced a confidence-modulated recognition system which learns to estimate its own confidence. Across a wide range of out-of-context datasets from our synthetic OCD dataset to real-world images, our model demonstrates superior performance over competitive baselines without retraining for each contextual condition, and exhibits human-like behavioral patterns over contextual variations. Despite great model performance, we also noted that there are still significant gaps between models and humans, particularly when recognizing small out-of-context objects.

References

- [1] Peter Battaglia, Razvan Pascanu, Matthew Lai, Danilo Jimenez Rezende, et al. Interaction networks for learning about objects, relations and physics. In *Advances in neural information processing systems*, pages 4502–4510, 2016. 2
- [2] Sara Beery, Grant Van Horn, and Pietro Perona. Recognition in terra incognita. In *Proceedings of the European Conference on Computer Vision (ECCV)*, pages 456–473, 2018. 2
- [3] Ali Borji, Saeed Izadi, and Laurent Itti. ilab-20m: A large-scale controlled object dataset to investigate deep learning. In *Proceedings of the IEEE Conference on Computer Vision and Pattern Recognition*, pages 2221–2230, 2016. 2
- [4] Wieland Brendel and Matthias Bethge. Approximating cnns with bag-of-local-features models works surprisingly well on imagenet. *arXiv preprint arXiv:1904.00760*, 2019. 2
- [5] Holger Caesar, Jasper Uijlings, and Vittorio Ferrari. Coco-stuff: Thing and stuff classes in context. In *Proceedings of the IEEE conference on computer vision and pattern recognition*, pages 1209–1218, 2018. 5, 7
- [6] Nicolas Carion, Francisco Massa, Gabriel Synnaeve, Nicolas Usunier, Alexander Kirillov, and Sergey Zagoruyko. End-to-end object detection with transformers. In *European Conference on Computer Vision*, pages 213–229. Springer, 2020. 3, 8
- [7] Liang-Chieh Chen, George Papandreou, Iasonas Kokkinos, Kevin Murphy, and Alan L Yuille. Deeplab: Semantic image segmentation with deep convolutional nets, atrous convolution, and fully connected crfs. *IEEE transactions on pattern analysis and machine intelligence*, 40(4):834–848, 2018. 2
- [8] Myung Jin Choi, Antonio Torralba, and Alan S Willsky. Context models and out-of-context objects. *Pattern Recognition Letters*, 33(7):853–862, 2012. 2
- [9] Wongun Choi and Silvio Savarese. A unified framework for multi-target tracking and collective activity recognition. In *European Conference on Computer Vision*, pages 215–230. Springer, 2012. 2
- [10] Jia Deng, Wei Dong, Richard Socher, Li-Jia Li, Kai Li, and Li Fei-Fei. Imagenet: A large-scale hierarchical image database. In *2009 IEEE conference on computer vision and pattern recognition*, pages 248–255. Ieee, 2009. 2, 3, 5
- [11] Zhiwei Deng, Arash Vahdat, Hexiang Hu, and Greg Mori. Structure inference machines: Recurrent neural networks for analyzing relations in group activity recognition. In *Proceedings of the IEEE Conference on Computer Vision and Pattern Recognition*, pages 4772–4781, 2016. 2
- [12] Santosh K Divvala, Derek Hoiem, James H Hays, Alexei A Efros, and Martial Hebert. An empirical study of context in object detection. In *Computer Vision and Pattern Recognition, 2009. CVPR 2009. IEEE Conference on*, pages 1271–1278. IEEE, 2009. 2
- [13] Alexey Dosovitskiy, Lucas Beyer, Alexander Kolesnikov, Dirk Weissenborn, Xiaohua Zhai, Thomas Unterthiner, Mostafa Dehghani, Matthias Minderer, Georg Heigold, Sylvain Gelly, et al. An image is worth 16x16 words: Transformers for image recognition at scale. *arXiv preprint arXiv:2010.11929*, 2020. 3, 8
- [14] Nikita Dvornik, Julien Mairal, and Cordelia Schmid. Modeling visual context is key to augmenting object detection datasets. In *Proceedings of the European Conference on Computer Vision (ECCV)*, pages 364–380, 2018. 2
- [15] Robert Geirhos, Patricia Rubisch, Claudio Michaelis, Matthias Bethge, Felix A Wichmann, and Wieland Brendel. Imagenet-trained cnns are biased towards texture; increasing shape bias improves accuracy and robustness. *arXiv preprint arXiv:1811.12231*, 2018. 2
- [16] Josep M Gonfaus, Xavier Boix, Joost Van de Weijer, Andrew D Bagdanov, Joan Serrat, and Jordi Gonzalez. Harmony potentials for joint classification and segmentation. In *Computer Vision and Pattern Recognition (CVPR), 2010 IEEE Conference on*, pages 3280–3287. IEEE, 2010. 2
- [17] Shirsendu Sukanta Halder, Jean-François Lalonde, and Raoul de Charette. Physics-based rendering for improving robustness to rain. In *Proceedings of the IEEE/CVF International Conference on Computer Vision*, pages 10203–10212, 2019. 2
- [18] Hexiang Hu, Guang-Tong Zhou, Zhiwei Deng, Zicheng Liao, and Greg Mori. Learning structured inference neural networks with label relations. In *Proceedings of the IEEE Conference on Computer Vision and Pattern Recognition*, pages 2960–2968, 2016. 2
- [19] Gao Huang, Zhuang Liu, Laurens Van Der Maaten, and Kilian Q Weinberger. Densely connected convolutional networks. In *Proceedings of the IEEE conference on computer vision and pattern recognition*, pages 4700–4708, 2017. 3, 5, 7, 8
- [20] Arthur Juliani, Vincent-Pierre Berges, Ervin Teng, Andrew Cohen, Jonathan Harper, Chris Elion, Chris Goy, Yuan Gao, Hunter Henry, Marwan Mattar, et al. Unity: A

- general platform for intelligent agents. *arXiv preprint arXiv:1809.02627*, 2018. 1, 2
- [21] Alex Krizhevsky, Ilya Sutskever, and Geoffrey E Hinton. Imagenet classification with deep convolutional neural networks. In *Advances in neural information processing systems*, pages 1097–1105, 2012. 2
- [22] Lubor Ladicky, Chris Russell, Pushmeet Kohli, and Philip HS Torr. Graph cut based inference with co-occurrence statistics. In *European Conference on Computer Vision*, pages 239–253. Springer, 2010. 2
- [23] Stephen C Mack and Miguel P Eckstein. Object co-occurrence serves as a contextual cue to guide and facilitate visual search in a natural viewing environment. *Journal of vision*, 11(9):9–9, 2011. 2
- [24] Spandan Madan, Timothy Henry, Jamell Dozier, Helen Ho, Nishchal Bhandari, Tomotake Sasaki, Frédo Durand, Hanspeter Pfister, and Xavier Boix. On the capability of neural networks to generalize to unseen category-pose combinations. *arXiv preprint arXiv:2007.08032*, 2020. 2
- [25] Jiteng Mu, Weichao Qiu, Gregory D Hager, and Alan L Yuille. Learning from synthetic animals. In *Proceedings of the IEEE/CVF Conference on Computer Vision and Pattern Recognition*, pages 12386–12395, 2020. 2
- [26] Aude Oliva and Antonio Torralba. The role of context in object recognition. *Trends in cognitive sciences*, 11(12):520–527, 2007. 2
- [27] Julia Peyre, Ivan Laptev, Cordelia Schmid, and Josef Sivic. Weakly-supervised learning of visual relations. In *ICCV*, 2017. 2, 5, 6, 7
- [28] Xavier Puig, Kevin Ra, Marko Boben, Jiaman Li, Tingwu Wang, Sanja Fidler, and Antonio Torralba. Virtualhome: Simulating household activities via programs. In *Proceedings of the IEEE Conference on Computer Vision and Pattern Recognition*, pages 8494–8502, 2018. 1, 2, 5
- [29] Shaoqing Ren, Kaiming He, Ross Girshick, and Jian Sun. Faster r-cnn: Towards real-time object detection with region proposal networks. *arXiv preprint arXiv:1506.01497*, 2015. 5, 7, 8
- [30] Amir Rosenfeld, Richard Zemel, and John K Tsotsos. The elephant in the room. *arXiv preprint arXiv:1808.03305*, 2018. 2
- [31] Krishna Kumar Singh, Dhruv Mahajan, Kristen Grauman, Yong Jae Lee, Matt Feiszli, and Deepti Ghadiyaram. Don’t judge an object by its context: Learning to overcome contextual bias. In *Proceedings of the IEEE/CVF Conference on Computer Vision and Pattern Recognition*, pages 11070–11078, 2020. 2
- [32] Jin Sun and David W Jacobs. Seeing what is not there: Learning context to determine where objects are missing. In *Proceedings of the IEEE Conference on Computer Vision and Pattern Recognition*, pages 5716–5724, 2017. 2
- [33] Hanlin Tang, Martin Schrimpf, William Lotter, Charlotte Moerman, Ana Paredes, Josue Ortega Caro, Walter Hardesty, David Cox, and Gabriel Kreiman. Recurrent computations for visual pattern completion. *Proceedings of the National Academy of Sciences*, 115(35):8835–8840, 2018. 6
- [34] Antonio Torralba. Contextual priming for object detection. *International journal of computer vision*, 53(2):169–191, 2003. 2
- [35] Antonio Torralba, Kevin P Murphy, and William T Freeman. Contextual models for object detection using boosted random fields. In *Advances in neural information processing systems*, pages 1401–1408, 2005. 2
- [36] Antonio Torralba, Kevin P Murphy, William T Freeman, and Mark A Rubin. Context-based vision system for place and object recognition. In *Computer Vision, IEEE International Conference on*, volume 2, pages 273–273. IEEE Computer Society, 2003. 2
- [37] Amazon Mechanical Turk. Amazon mechanical turk. Retrieved August, 17:2012, 2012. 5
- [38] Ashish Vaswani, Noam Shazeer, Niki Parmar, Jakob Uszkoreit, Llion Jones, Aidan N Gomez, Lukasz Kaiser, and Illia Polosukhin. Attention is all you need. *arXiv preprint arXiv:1706.03762*, 2017. 3, 8
- [39] Kevin Wu, Eric Wu, and Gabriel Kreiman. Learning scene gist with convolutional neural networks to improve object recognition. In *Information Sciences and Systems (CISS), 2018 52nd Annual Conference on*, pages 1–6. IEEE, 2018. 2
- [40] Jian Yao, Sanja Fidler, and Raquel Urtasun. Describing the scene as a whole: Joint object detection, scene classification and semantic segmentation. In *Computer Vision and Pattern Recognition (CVPR), 2012 IEEE Conference on*, pages 702–709. IEEE, 2012. 2
- [41] Mengmi Zhang, Claire Tseng, and Gabriel Kreiman. Putting visual object recognition in context. In *Proceedings of the IEEE/CVF Conference on Computer Vision and Pattern Recognition*, pages 12985–12994, 2020. 2, 4, 5, 6, 7, 8